Video Article

Assessing Collagen and Elastin Pressure-dependent Microarchitectures in Live, Human Resistance Arteries by Label-free Fluorescence Microscopy

Maria Bloksgaard[1], Bjarne Thorsted[2], Jonathan R. Brewer[2], Jo G. R. De Mey[1,3]

[1]Department of Cardiovascular and Renal Research, Institute of Molecular Medicine, University of Southern Denmark

[2]Department of Biochemistry and Molecular Biology, University of Southern Denmark

[3]Department of Cardiac, Thoracic and Vascular Surgery, Odense University Hospital

Correspondence to: Maria Bloksgaard at mbloksgaard@health.sdu.dk

URL: https://www.jove.com/video/57451
DOI: doi:10.3791/57451

Keywords: Bioengineering, Issue 134, Two-photon excitation fluorescence microscopy, extracellular matrix, image analyses, resistance arteries, Ilastik, Fiji, microstructure, mechanics, mathematical modeling

Date Published: 4/9/2018

Citation: Bloksgaard, M., Thorsted, B., Brewer, J.R., De Mey, J.G. Assessing Collagen and Elastin Pressure-dependent Microarchitectures in Live, Human Resistance Arteries by Label-free Fluorescence Microscopy. *J. Vis. Exp.* (134), e57451, doi:10.3791/57451 (2018).

Abstract

The pathogenic contribution of resistance artery remodeling is documented in essential hypertension, diabetes and the metabolic syndrome. Investigations and development of microstructurally motivated mathematical models for understanding the mechanical properties of human resistance arteries in health and disease have the potential to aid understanding how disease and medical treatments affect the human microcirculation. To develop these mathematical models, it is essential to decipher the relationship between the mechanical and microarchitectural properties of the microvascular wall. In this work, we describe an *ex vivo* method for passive mechanical testing and simultaneous label-free three-dimensional imaging of the microarchitecture of elastin and collagen in the arterial wall of isolated human resistance arteries. The imaging protocol can be applied to resistance arteries of any species of interest. Image analyses are described for quantifying i) pressure-induced changes in internal elastic lamina branching angles and adventitial collagen straightness using Fiji and ii) collagen and elastin volume densities determined using Ilastik software. Preferably all mechanical and imaging measurements are performed on live, perfused arteries, however, an alternative approach using standard video-microscopy pressure myography in combination with post-fixation imaging of re-pressurized vessels is discussed. This alternative method provides users with different options for analysis approaches. The inclusion of the mechanical and imaging data in mathematical models of the arterial wall mechanics is discussed, and future development and additions to the protocol are proposed.

Video Link

The video component of this article can be found at https://www.jove.com/video/57451/

Introduction

The pathogenic contribution and effects of resistance artery remodeling are documented in essential hypertension, diabetes and the metabolic syndrome[1,2,3,4,5]. Deciphering the relationship between the mechanical and microarchitectural properties of the microvascular wall is essential for developing mathematical models of this association. Such models will improve understanding the remodeling process and will support the development of in silico models useful for testing pharmacological strategies targeting disease related remodeling of the arterial wall.

Prior studies focused in understanding how the microarchitecture of the arterial wall relates to arterial wall mechanics by incorporating mechanical measures and the microarchitecture of the extracellular matrix (ECM) are almost exclusively performed on large, elastic conduit arteries from mice or swine[6,7,8,9,10,11]. Imaging of the microstructures of the wall is typically performed using nonlinear optical techniques, taking advantage of the autofluorescence of elastin and second harmonic generation by collagen. This allows spatiotemporal imaging of the two major components of the extracellular matrix, elastin and collagen, without a need for staining. Imaging of the arterial wall in full thickness is a challenge in large conduit arteries due to scatter of the light in the thick tunica media. However, to determine how the microarchitecture of the structural components of the arterial wall relate to the observed mechanical properties, three-dimensional information must be obtained during the mechanical testing. For large arteries like the human aorta, this requires biaxial mounting, mechanical testing and imaging of regions of interest in 1-2 cm^2 pieces of the arterial wall[7,9,10,12]. Only part of the wall can be imaged and mechanically tested.

For smaller arteries of any species (*e.g.*, human pericardial[13], pulmonary[14] and subcutaneous[15] arteries, rat mesenteric arteries[16,17,18,19,20], mouse cremaster, mesenteric, cerebral, femoral and carotid arteries[21,22,23,24,25,26,27]) imaging of the entire wall thickness is possible and can be combined with mechanical testing. This allows simultaneous recording of the mechanical properties and the structural arrangements within the wall. However, a direct mathematical modeling of the relationship between the observed alterations in the three-dimensional structure of the ECM and changed mechanical properties of the resistance arterial wall, has to the best of our knowledge only been reported upon recently in human resistance arteries[13,15].

In this work, an *ex vivo* method for passive mechanical testing and simultaneous three-dimensional imaging of the microarchitecture of elastin and collagen in the arterial wall of isolated human resistance arteries is described. The imaging protocol can be applied to resistance arteries of any species of interest. Image analyses are described for obtaining measures of internal elastic lamina branching angles and adventitial collagen straightness[13] using Fiji[28]. Collagen and elastin volume densities are determined using Ilastik software[29] and finally, the inclusion of the mechanical and imaging data in mathematical models of the arterial wall mechanics is discussed.

The goal of describing the imaging and image analyses techniques in combination with mathematical modeling is to provide investigators a systematical approach to describe and understand observed pressure induced changes in the ECM of resistance arteries. The described method is focused in quantifying the changes in the ECM in a vessel during pressurization, by comparing the structure of the ECM at 20, 40 and 100 mmHg. These pressures were chosen for determining the structure of the arterial wall at its more compliant (20 mmHg), stiff (100 mmHg) and intermediate (40 mmHg) state, respectively. However, any process in the vascular wall of live arteries, including changes induced by vasoactive components, hysteresis and flow, can be quantified, depending on the research hypothesis in question by the investigator.

The use of two-photon excitation fluorescence microscopy (TPEM) in combination with a pressure myograph for studying pressure (or other) induced changes in the ECM of live arteries is emphasized. First, because this allows simultaneous acquisition of the overall three-dimensional structure of the arterial wall (diameter and wall thickness) along with three-dimensional label-free acquisition of high quality, detailed images of the collagen and elastin microarchitectures as described[13] by taking advantage of the elastin autofluorescence and the collagen second harmonic generation signal (SHG)[30]. Second, TPEM allows use of low-energy near-infrared excitation light, minimizing photodamage of the tissue and thus, repeated imaging at exactly the same position within the vascular wall is allowed, permitting repeated-measurements analyses of observed changes.

The use of an alternative approach using confocal imaging of pressure fixed arteries is discussed to allow users without access to TPEM an opportunity to use the described method as well. Information on ECM structure and volume densities can also be retrieved from two-dimensional analyses of tissues sectioned in serial, e.g. as described by[31,32]. However, due to the lack of possibility to retrieve three-dimensional structural information over the length scales of the artery as well as during changing conditions using this method, it is not recommend using this approach for investigations of pressure and treatment induced three-dimensional changes in the ECM.

The minimum requirement for the investigator to apply the herein described method is the access to a setup for cannulation and pressurization of arteries in combination with a confocal or two-photon excitation fluorescence microscope. The setup described in the following protocol is a custom-built pressure myograph with a longitudinal force transducer, built to fit on a custom built inverted two-photon excitation fluorescence microscope.

Protocol

Collection of biopsies of the human parietal pericardium for use in this work was performed after written informed consent, as previously described[33]. The study of human tissues conform to the principles outlined in the Declaration of Helsinki[34] and was approved by The Regional Committees on Health Research Ethics for Southern Denmark (S-20100044 and S-20140202) and the Danish Data Protection Agency.

1. Collect Tissue and Isolate (Human) Resistance Artery

1. Collect tissue samples of interest immediately upon the excision during a surgery. Transfer the tissue to 4 °C HEPES buffered physiological salt solution (HBS) immediately upon collection and store it in HBS.
   NOTE: Human tissues are only collected following approval by relevant institutional and ethical committees as well as patients' written informed consent. HBS composition in mM: NaCl 144, KCl 4.7, $CaCl_2$ 2.5, $MgSO_4$ 1.2, KH_2PO_4 1.2, HEPES 14.9, glucose 5.5. Adjust the pH 7.4 with NaOH, and filter the solution though 0.2 µm filter.
2. Leave the collected tissue in sterile HBS at 4 °C overnight to wash out anesthetics.
   NOTE: Any effect of overnight storage on vessel integrity and functionality should be checked by the individual research laboratory.
3. Carefully isolate resistance sized arteries (± 200 µm lumen diameter) using a pair of sharp-tip forceps and micro-dissection scissors.
4. Store the arteries at 4 °C in ice-cold HBS while priming the imaging/pressure chamber.

2. Mount the Isolated Artery in the Pressure Myograph

1. Mount the glass cannulae with tip diameters of ~80 µm on cannulae holders. Position the tips approximately 150 µm above the chamber glass bottom.
   NOTE: 45° bended tip cannulae may allow precise positioning of the vessel above the glass bottom.
2. Fill both inlet and outlet tubing with HBS with 1% BSA and connect to the pressure system.
   NOTE: BSA is included to preserve endothelial cell function.
3. Mount the isolated artery using two double knot sutures per cannula.
   NOTE: Knots can be prepared in advance and stored on double adhesive tape until needed.
4. Fill the chamber with HBS and place two double knots on each glass cannula.
   NOTE: When using arteries displaying myogenic tone, HBS should be replaced with calcium free HBS supplemented with 3 µM EGTA and 3 µM sodium nitroprusside.
5. Hold the artery gently at one end using two pairs of sharp tip forceps. Open the lumen of the artery and gently slide it onto the cannula. Fix on cannula using two knots.
6. Apply a pressure of 5 mmHg to gently flush the lumen with HBS / 1% BSA.
7. Cannulate the other end of the artery and secure it on the cannula using two double knots.
8. Transfer the myograph to the microscope stage and pressurize the artery to 5 mmHg (inlet pressure = outlet pressure), then heat to 37 °C for 30 min.

9. Optional: Calibrate the longitudinal force transducer according to the manufacturer's instructions (1 g = 9.81 mN).
NOTE: It is essential to calibrate the force transducer after heating as it is temperature sensitive.

3. Perform Experiment: Imaging of Arterial Diameter, Wall Thickness and Collagen and Elastin Microarchitecture Using TPEM

1. Quickly scan the cannulated artery pressurized to 5 mmHg using a 20X objective (numerical aperture (NA) ≥ 0.8) and low power excitation light to assess vessel diameter and wall thickness at 5 mmHg.
NOTE: For inverted microscopes, use a water immersion objective; for upright microscopes, use a water dipping objective. If the objective does not have a correction collar to correct for cover slip thickness, make sure to match the used cover slip with the objective used. The software settings and descriptions may vary depending on the user-interphase and microscope and software used.
    1. Setup the optical path.
        1. Activate Mai Tai two-photon laser and set it to 820 nm excitation light.
        CAUTION: Avoid any exposure to visible as well as invisible laser light.
        2. Collect emission simultaneously in two channels. Split emission light between the photomultipliers using a 460 nm long pass dichroic mirror and collect emission using 30-60 nm wide bandpass filters centered at 520 nm (elastin) and 410 nm (collagen), respectively.
    2. Enable continuous scanning with 10 µs laser dwell time/pixel and 512 × 512 pixels for 100% field of view.
    3. Manually scan through the artery to determine the depth where maximum diameter is observed.
    4. Choose a rectangular slice covering the artery's widest diameter and scan a single frame with pixel size ≤ 300 nm/pixel (**Figure 2C**). Use as low excitation light power and pixel dwell time as possible to avoid photodamaging the live artery.
    NOTE: It is recommended to obtain a rectangular, *e.g.*, 100 × 1024 pixel image, rather than quadratic image at this position to save time and limit the tissue photon exposure (**Figure 2C**).
    5. Save the image for later analyses.

2. Determine lumen diameter and wall thickness at the maximum diameter of the artery.
    1. Load the image in Fiji.
    2. Set the scale by clicking **Main menu | Analyze | set scale** and enter µm/pixel and pixel ratio (it is highly recommended to keep the pixel ratio 1:1).
    3. Choose the Fiji **line** tool and draw a line between the two internal elastic laminae at each side of the arterial lumen, and click **ctrl + M**. Fiji reports length as default in the results table.
    4. Likewise, draw more lines to measure thickness of each wall, and click **ctrl + M** to measure the following markup.
    5. Save the measurements.

3. Image collagen and elastin microarchitecture at 5 mmHg by scanning the entire thickness of the arterial wall, obtaining 3D image stacks with good quality for 1-3 regions of interest along the length of the artery.
    1. Obtain image stacks through the entire wall of the artery using a 60X objective, NA ≥ 1, optimized pixel sizes and z-spacing.
        1. Calculate the optimal imaging conditions (pixel sizes and z-step spacing) in accordance with the optical pathway, immersion medium and sample refractive indices using the Scientific Volume Imaging Nyquist calculator (https://svi.nl/NyquistCalculator).
        NOTE: Please pay attention here to the difference between optimal pixel size and z-spacing versus the advice in section 3.4. above on the use of a *maximum* pixel size.
    2. Use the same excitation and emission settings as above (3.1.1.).
    3. Quickly scan the vessel wall as described above to determine the thickness of the z-stack.
    4. Define the z-stack start and end depth, z-step spacing and pixel density (calculated in 3.3.1.1.) and perform the z- scan. Save each channel separately.
    NOTE: Images should be small enough *e.g.* 30 x 30 µm or 50 × 50 µm depending on the vessel size to avoid any influence of curvature in the subsequent image analyses.

4. Determine arterial diameter, wall thickness, and elastin and collagen microarchitecture at remaining pressures of protocol.
    1. Repeat 3.1-3.2 at pressures 10 and 20 mmHg, repeat 3.3 at pressure 20 mmHg.
    2. Repeat 3.1 and 3.2 at pressure 40 mmHg.
    3. Repeat 3.1-3.2 at pressures 60, 80, and 100 mmHg and repeat 3.3 at 100 mmHg.
    NOTE: 3.1-3.3 can be repeated for all pressures, and combinations of pressures (e.g. a series/combination of increasing as well as decreasing pressures), depending on the hypothesis to be tested. Eosin in concentration 0.3 - 1 µM may be added to enhance elastin autofluorescence in case of photobleaching. Photobleaching can be avoided by applying as low power excitation light as possible.
    4. Replace the buffer in the myograph chamber with fresh 37 °C HBS after each pressure step. Allow the artery to adapt for 5 min prior to imaging following each change in pressure.

5. Store channel stacks separately for image analyses.
6. Test viability of the artery.
    1. Apply 10 µM U46619 in the myograph chamber followed by the addition of 10 µM bradykinin when a stable constriction is observed.
    2. Record diameter and wall thickness as described above in section 3.1 following the application of each of the compounds.
    3. Add 3 µM sodium nitroprusside when the artery is not fully dilated following the addition of bradykinin and record diameter and wall thickness.
    NOTE: Depending on the pharmacological properties of the artery of interest (vascular bed and species) other vasoconstrictor and (endothelium-dependent) vasodilator compounds can be used.

7. Optional: Fix the pressurized artery or continue with imaging of collagen and elastin for volume densities (step 7).

1. Add 4% formaldehyde in 1x phosphate-buffered saline (PBS) at 37 °C for 1 h.
2. Wash the fixed artery three times in 1x PBS and gently slide the artery off the cannulae, touching only the parts of the artery outside the knots. Do not remove the knots, use them for holding the artery when transferring to a storage tube.
3. Store in 1x PBS / 0.05 % sodium azide at 4 °C until imaging for elastin and collagen volume densities or other purposes.
   NOTE: Fixed arteries can be stored for at least 3 months in 1x PBS / 0.05 % sodium azide at 4 °C.

4. Calculation of Stress Strain Relationships and Intrinsic Wall Stiffness

1. Please follow the formulas and calculation steps for calculating stresses, strains, and wall stiffness as described by Bloksgaard, M. *et al.*[13] and references herein.

5. Image Analysis - (Internal Elastic Lamina) IEL Branching Angles

1. Open image stack in Fiji. Go to **file | open image** to choose image stack.
   NOTE: Max intensity projections of 2-7 consecutive z-sections covering the IEL (1-2 µm thickness) are used for determining the IEL elastin fiber branching angles using the angle tool in Fiji[28,35]. Refer to **Figure 4A** for illustration.
2. Go to **Image | stacks | z project…** to choose the images and "Max Intensity Projection".
3. Save the max intensity projection as TIFF.
4. Choose as many IEL fiber branching points as possible using the "angle tool", and work systematically through the images. Click **ctrl + M** to measure each angle.
5. Save the Fiji results sheet.

6. Image Analysis - Adventitial Collagen Waviness

1. Open image stack in Fiji. Go to **file | open** image to choose image stack.
   NOTE: Max intensity projections of 2-7 consecutive z-sections covering collagen right outside the external elastic lamina (EEL, 1-4 µm thickness) are used for determining collagen waviness using the Fiji NeuronJ plugin[36] as described by Rezakhaniha, R. *et al*.[37](**Figure 4B**).
2. Set the scale. Go to **analyze | set scale** to enter pixel dimensions.
3. Go to **Image | stacks | z project…** to choose images to work with and "Max Intensity Projection".
4. Change Image type to 8 bitt TIFF by clicking **Image | type | 8 bitt** and save the max intensity projection as TIFF.
5. Measure collagen fiber straightness using the Fiji Neuron J Plugin.
   1. Open the NeuronJ plugin by clicking **Fiji | Plugins | Neuron J**.
   2. Open the 8bit TIFF in NeuronJ by clicking **Load Image | Select File**.
   3. Click **add tracings**, and select fibers to analyze by clicking on start and end of each fiber.
   4. Click **Measure tracings**, choose **display tracing** (Lf) and **vertex measurements** in the dialog box.
6. Calculate L0/Lf in excel (or similar) and save the results.
   1. Copy and paste Fiji Neuron J tracings and vertices output to excel (or similar) and calculate L0 using Pythagoras's theorem from the vertex measurements. First and last point on line indicate the positions of the ends of the hypotenuse in a 2D coordinate system.
      NOTE: A L0/Lf [collagen fiber bundle end-to-end length via a straight line (L0) / full length (Lf)] close to 1 indicates an almost straight collagen fiber.

7. Imaging for Collagen and Elastin Volume Densities

1. Wash the (fixed) artery 1x in PBS and stain it for 15 min in 1 µM eosin in 1x PBS in the dark. For fixed arteries, perform this step at room temperature.
   NOTE: Eosin enhances the elastin fluorescence. Eosin will stain other structures such as collagen and the cell cytoplasm if the sample is left in the staining solution for extended time. If staining of other structures is too intense, lower the concentration of eosin to 0.3 µM or repeat washing.
2. Wash the artery 3x in 1x PBS
   1. For fixed arteries: mount the artery for imaging.
      Caution: Imaging of non-pressurized vessels does not allow retrieval of any geometrical quantitative information. When absolute quantities are required, these should always be obtained on live, pressurized arteries. Volume-ratios can be obtained on the non-pressurized arteries with this method.
      1. Place two pieces of double adhesive tape 1-1.5 cm apart on an object glass. Double adhesive tape is approximately 100 µm thick. Apply one or more layers of tape to match the diameter of the artery to be mounted.
      2. Place 10-20 µL of PBS on the glass in the middle of the square and place the artery in the PBS drop.
         NOTE: The drop should be as small and flat as possible to avoid pushing the artery out of position when mounting the cover slip.
      3. Place the coverslip and press onto double adhesive tape.
      4. Fill the reservoir between the coverslip and object glass with 1x PBS. Refill it every hour to avoid drying of the sample.
3. Obtain image-stacks for collagen and elastin volume densities using a 20X objective with NA > 1 to cover as much of the arterial wall as possible while still having a good optical resolution (**Figure 2D**, **2G and 2H**).
   NOTE: Use a water immersion objective for imaging of fixed arteries under a coverslip, and use a water dipping objective for imaging of vital arteries. If the objective does not have a correction collar to correct for cover slip thickness, make sure to match the coverslip to the objective.

Preferably use optimal pixel sizes and z-spacing. Calculate these using the Nyquist Calculator (step 3.3.1.1.). Alternatively, use a minimum pixel size of 300 nm and z-spacing of 1 µm. It is recommended to obtain three images along the length of the artery to allow the user to determine intra-assay variability.
4. Image elastin using 820 nm excitation light and collect emission using a 30-60 nm wide bandpass filter centered at 520 nm.
5. Image collagen using 990 nm excitation light to avoid any excitation of elastin and other autofluorescent proteins and collect emission using 10-30 nm wide bandpass filter centered at 495 nm.
6. Save image stacks from each channel separately as TIFF files

8. Image Analysis for Extracting Elastin and Collagen Volume Densities Using Ilastik

1. Convert TIFF image stacks to HDF5 using Fiji[28,35] by clicking Choose **File | Save As… HDF5**.
2. Create two data file folders on the computer hard drive, one for elastin, one for collagen image stacks, respectively. Copy relevant image stacks to the relevant folder.
3. Create two new Ilastik projects in the Ilastik software, one of elastin, one for collagen, respectively.
    1. Open **Ilastik | Create new project | pixel classification | new project | add data** and select image folder created in step 8.2.
    NOTE: Follow the Ilastik wizard.

4. Import one 3D image stack to train the software.
    1. Select the **Input Data applet | main workspace area | Raw Data tab | Add new … | Add separate Image(s)** and choose the desired image data

5. Choose relevant features in the software.
    1. Open **Feature Selection applet | Select Feature** which opens a new dialog. See **Figure 5A** for details.

6. Add at least two labels using the **Add Label** button under the Training applet.
NOTE: Each label will correspond to an object type that needs to be separated. In this work, three labels are used for elastin: elastin itself, bright spots (to be excluded), and background (to be excluded).
7. Draw labels on top of the raw image stack using the paint brush styled annotation tool.
    1. Select the appropriate label: click **brush** tool and start drawing.

8. Prompt Ilastik to analyze the image stack and look for similar features by clicking **Enable Live Update**.
9. Check carefully the prediction map (**Figure 5D**).
NOTE: The process from raw image to a complete prediction map is shown in **Figure 5**. Ilastik uses the prediction map to segment the image stack according to which label a pixel is more likely to be associated (**Figure 5D**).
10. Apply a threshold.
    1. Select **Thresholding applet**, choose an appropriate method, input label, smooth, threshold and size filter parameters, and finally click Apply.
    NOTE: This segregates the similarly labeled parts of the image into discrete objects. Highly connected tissue, like elastin and collagen does not need to be segregated, therefore, a threshold of 0.4 is applied (the default is 0.5). **Figure 5E** and **5F** illustrate the result of applying a threshold.

11. Repeat the training of Ilastik until the outcome is satisfactory (only elastin, respectively collagen is recognized for the respective analyses).
    1. Frequently switch between the Training and Segmentation (and sometimes also the Thresholding) applets during this process. An example of the effect of re-training Ilastik is shown in **Figure 6**.

12. Batch analyze similar image data: select **batch prediction input selection** and add relevant files.
NOTE: The Ilastik output is a collection of pseudo-1bit 3D image stacks (image masks) with 0 (zero) denoting the absence of elastin (or collagen) and 1 (one) denoting the presence hereof (The actual bit depth is 8-bit).
13. Verify the results for each image stack by visually comparing the image masks and the raw image files.
14. Optimize the Ilastik mask (steps 8.4-8.9) and re-analyze any image stacks with unsatisfactory results.
15. Calculate elastin and collagen volume densities from Ilastik image masks using MATLAB
    1. Open **MATLAB**.
    2. Select folder with ilastik image masks in MATLAB "current folder" window.
    3. Copy the MATLAB script from **Supplementary File 1** to the MATLAB editor and save the code as volumeCalculator.m in the MATLAB folder on the computer hard drive.
    4. Enter pixel sizes and pixel height in the script lines
    pixelSize = 0.1230000*0.1230000; %micron*micron
    pixelHeight = 0.9; % micron
    5. Save the script.
    6. Go to MATLAB command window and enter "volumeCalculator('path-to-data')"to load the script.
    7. Click enter. Each Image mask is now summed up and multiplied by the (known) pixel/voxel volume (physical dimensions of a pixel multiplied by the z-axis resolution). The output from MATLAB is the total volume of elastin and collagen in each image stack.

16. Save the results.

Representative Results

The custom-built pressure myograph for imaging used in this work is shown in **Figure 1**. Special attention for the design of the myograph was paid to i) the chamber with a small volume (2 mL) and ii) the possibility for positioning the cannulae close to, and parallel with the glass bottom (**Figure 1B**). The bottom of the chamber fits a 50 × 24 mm #1.5 glass coverslip (replaceable). The pressure controller was built from a standard 1 L glass bottle and a sphygmomanometer (cuff removed). For a myograph setup with flow requirements, the use of a servo pressure controller is recommended.

Figure 2 illustrates the recommended positions for obtaining single images and image stacks during the experiment outlined in the protocol. For illustration purposes, a transmission light microscopy image of the mounted artery is included in **Figure 2A**. Knot-to-knot length of the mounted artery is approximately 1.6 mm. The artery is scanned until the widest diameter is observed (**Figure 2B**), and at this point, the diameter and wall thickness are determined (**Figure 2C**). Likewise, a transmission light image of the artery is included in **Figure 2D**, showing the position and recommended width of the image stacks for determining the microarchitectures of collagen (**Figure 2E**) and elastin (**Figure 2F**, small square in **Figure 2D**) as well as the image stacks for determining the collagen (**Figure 2G**) and elastin (**Figure 2H**) volume densities (larger square, **Figure 2D**). Using this approach, data for constructing pressure diameter curves, followed by the calculation of the corresponding stress-strain curves can be obtained from pressure, diameter and wall thickness measurements (**Figure 2C**).

A single exponential fit of the stress-strain relationship according to Bloksgaard *et al.*[13] and references herein, provides the β-value, a geometry independent measure of wall stiffness proportional to the incremental elastic modulus, E_{inc}. Calculating E_{inc} at the different pressures at which images for collagen and elastin microarchitectures were obtained, allows a direct analysis of the relationship between the pressure induced changes in the microarchitectures of collagen and elastin and the incremental elastic modulus at different pressures (**Figure 3**). The measurement of IEL branching angles and collagen straightness is illustrated in **Figure 4**.

Important for the interpretation of mechanical data comparing two or more groups of interest, *e.g.* hypertensive vs normotensive patients, is a determination of the content of elastin and collagen. For this, an automatic analysis method in Ilastik, a freeware image analysis software that can be trained to recognize certain image features, was developed. The work-flow in Ilastik is illustrated in **Figure 5**.

For the automatic detection of elastin and collagen for the volume densities, it is important that there is a good signal-to-noise ratio in the images obtained. In human samples, significant autofluorescence from collagen is often observed in addition to the collagen SHG signal. This decreases the signal-to-noise ratio for the detection of elastin. **Figure 6** illustrates how re-training of the Ilastik program can result in better recognition of thin elastin fibers in a sample with significant collagen autofluorescence in the "green"/elastin channel. If bleed-through of the autofluorescence signal into the collagen SHG channel is a problem, obtaining the SHG signal using a longer excitation wavelength may help. If the channel bleed through occurs after staining with eosin, the concentration of the applied solution of eosin should be lowered. Eosin is easily washed out, so repeated washing of the stained sample may decrease the signal too.

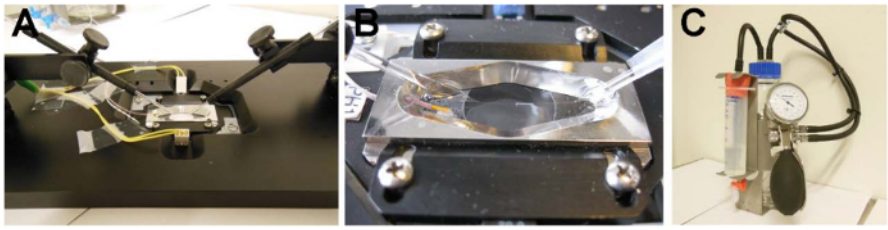

Figure 1. Custom built pressure myograph for fluorescence imaging. (A) Perfusion chamber with glass capillaries attached to the micromanipulators, which is mounted on a force transducer (longitudinal force). (B) 2 mL imaging chamber. The 45° bending of the cannulae facilitates imaging using an inverted microscope. (C) Pressure controller. Please click here to view a larger version of this figure.

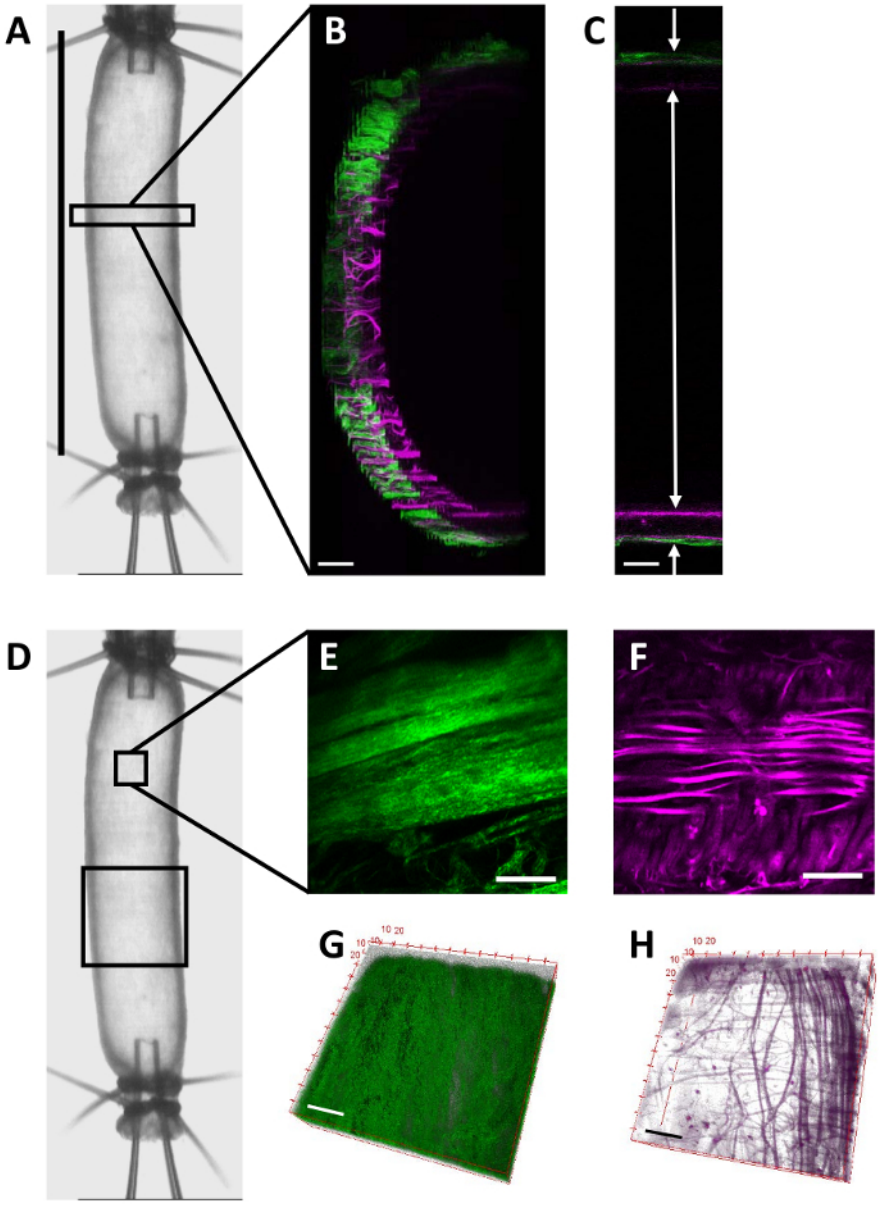

Figure 2. Combined pressure myography and fluorescence imaging strategy. (A) Transmission light image of the artery with illustration of (B) the scan of the full width of the artery. The collagen SHG is shown in green, and elastin autofluorescence in magenta. (C). Arterial lumen diameter (here 238 µm) and wall thicknesses (here 17 and 18 µm top and bottom, respectively) is determined at the equatorial region (largest diameter observed) of the artery. (D) Transmission light image of the artery with the illustration of the position of the z-stacks obtained at a 10-50 µm scale for determining (E) collagen straightness, (F) branching angles of the internal elastic laminae, and (G) z-stacks obtained at a 50-100 µm scale for obtaining collagen and (H) elastin volume densities. Images B/C: height 300 µm (bar 20 µm), E/F: 50 x 50 µm (bar 10 µm), G/H 130 × 130 × 30 µm (bar = 30 µm). Please click here to view a larger version of this figure.

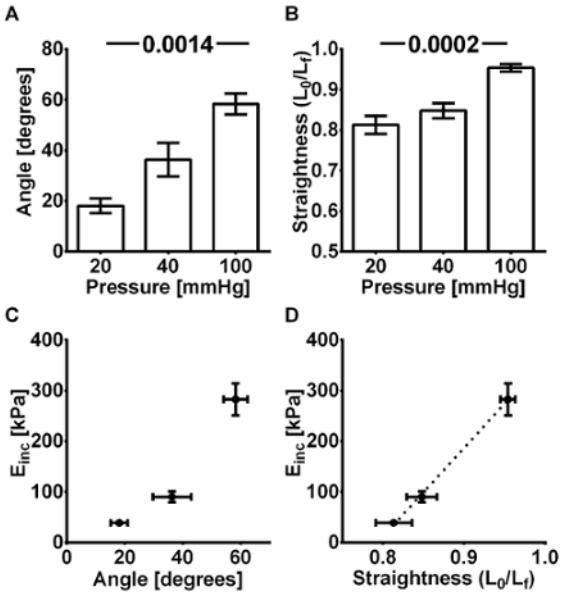

Figure 3. Microstructural changes in adventitial collagen and the internal elastic lamina (IEL) and their relation to the circumferential incremental elastic moduli at 20, 40 and 100 mmHg. (A) Branching angles of elastin fibers in the IEL. (B) Straightness of adventitial collagen fibers close to the external elastic lamina. *p*-values and according F-values were determined using repeated measurements one-way ANOVA: *p*/F-values A: 0.0014/24.18, B: 0.0002/37.38. (C) IEL branching angles correlates nonlinearly with E_{inc}. (D) Collagen straightness correlates linearly with E_{inc}. Data are shown as mean ± SE. Microstructural changes (A and B, and x-axes of C and D) were determined for 6 resistance arteries subjected to vital imaging while E_{inc} (C and D) was calculated for 20 other arteries subjected to pressure myography in a standard pressure myograph. Each artery studied was from a different individual. This figure has been modified from Bloksgaard *et al.*[13]. Please click here to view a larger version of this figure.

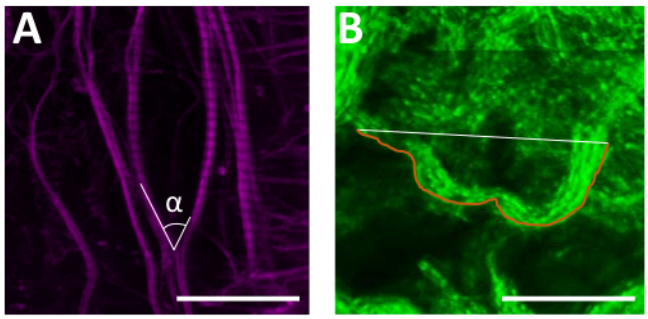

Figure 4. Illustration of measurements of IEL branching angles and collagen straightness in Fiji. (A) IEL branching angles are manually marked and measured using the Fiji angle tool. (B) Collagen straightness is determined using the Fiji Neuron J plugin as the ratio of the end-to-end length of a single collagen fiber via a straight line (white) divided by the actual end-to-end length of the fiber (orange). Bar size: 20 µm.

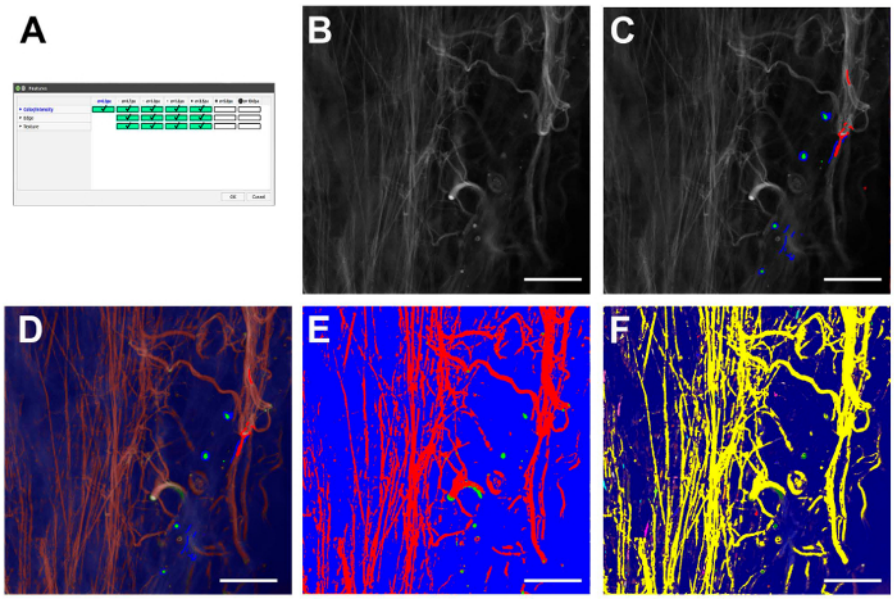

Figure 5. Ilastik workflow. (A) Feature selection window with the indication of selected features. (B) Example raw image with (C) labels for elastin fibers, bright spots (undesired) and background highlighted in red, green and blue, respectively. (D) Resulting prediction map for image (B) with labels indicated in (C). (E) Segmentation based on the prediction map in (D) before (E) and after (F) applying a threshold of 0.5. Yellow color shows the connected pixels corresponding to the segregated feature (elastin). Bar size: 25 µm. Please click here to view a larger version of this figure.

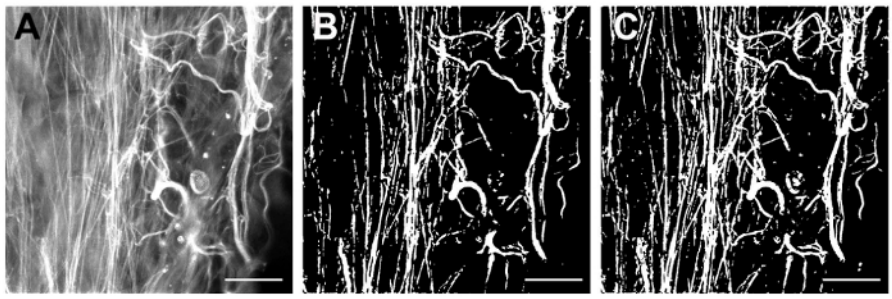

Figure 6. Example images before and after the optimization of the Ilastik prediction map showing the effect of re-training Ilastik for recognition of elastin fibers in a sample with high background fluorescence from collagen (sub-optimal signal to noise ratio). (A) Original image, (B) result of first Ilastik analysis, where especially the thin elastin fibers (left side of image B) are not included in the segmentation and (C) final result following the optimization of the prediction map. Bar size: 25 µm. Please click here to view a larger version of this figure.

Supplementary File Please click here to download this file

Discussion

This work represents our suggestion for a standardized, combined imaging and pressure myography approach, valuable for simultaneous assessment of the mechanical properties of resistance arteries and pressure-related changes in the structure of the arterial wall over a pressure range from 0 to 100 mmHg. The presented approach was developed using custom built equipment, however, any pressure myograph that fits on a two-photon excitation fluorescence microscope can be used, when the design of both equipments allows imaging of the arterial wall. Special attention should be paid to the shape, width and working distance of the objective, and the conditions under which the imaging will be performed. Upright microscopes require the use of water dipping objectives, whereas the use of water immersion objectives is recommended for inverted microscopes to avoid differences in refractive indices between the sample and the objective. Furthermore, attention should be paid to the coverslip thickness, either by applying a correction for a mismatch between the objective and coverslip using the correction collar on the objective (if present) or by matching the coverslip thickness with the objective used.

In the described protocol, advantage is taken of low-energy, near-infrared light for imaging elastin autofluorescence and collagen SHG. This allows imaging for extended periods of time. In the human resistance arteries used in this study, the IEL is comprised of a longitudinally aligned fiber-like network of interconnected elastin fibers[13,33], similar to the structure of the IEL of human subcutaneous resistance arteries (hSCA)[38,39]. Changes in branching angles of the elastin fibers in the IEL were evaluated and used together with measures of the gradual uncoiling of adventitial collagen fibers with increasing pressures[37] to assess changes in the microarchitecture of elastin and collagen respectively. Images for assessing elastin and collagen microarchitectures were obtained at the same region of interest within the arterial wall at different pressures. This allows repeated-measurements analyses. When possible, the investigator could aim at obtaining images in at least 3 regions of interest, with image sizes 10-50 µm in each dimension. However, depending on the sample, especially the thickness of the arterial wall, a compromise

has to be made between the number of scanned regions of interest and the feasible duration of the experiment. In case of the human pericardial resistance arteries, the arteries remained alive for at least 8-12 h of experimentation. Scanning several regions of interest allows evaluation of intra- versus inter-sample variability and thus supports the conclusion on the obtained findings.

It is important to notice that to avoid inducing phototoxic damage, imaging using high power excitation light should be avoided when working on live tissue specimens. In light of this, it is recommended to obtain the large image stacks for collagen and elastin volume densities at the end of the experimental protocol, alternatively on fixed samples. When absolute quantities of the ECM components are required, any effect of the fixative on the volume densities should be quantified and taken into account. Fixation and permeabilization of the arteries allows furthermore staining of intracellular targets of interest when necessary. In this protocol, staining for elastin is performed using eosin on the live artery. Staining of elastin by specific probes (*e.g.,* alexa 633 hydrazide[40]) and collagen (*e.g.,* CNA35[41]), may be applied together with other stains (*e.g.,* phalloidin[42]) or DNA, to facilitate the assessment of volumetric densities and structural organization of other structures of interest in the arterial wall. This opportunity may provide research laboratories with single-photon confocal microscopes an opportunity to investigate the microstructural changes in resistance arteries. Segments from the same artery may be treated under different conditions, fixed under pressure and imaged at a later stage to compare the effect of the applied treatment. Targets of interest should be visualized by imaging the re-cannulated, re-pressurized and stained vessels. Re-cannulation and re-pressurization is required when structural changes are considered, as elastin cannot be fixed and hence will recoil and alter the 3D structure of the fixed artery[43,44]. The drawback of determining structural changes in fixed arteries is that several segments have to be fixed for comparison, and repeated-measurement analyses cannot be performed.

The data obtained using imaging can be directly used to calculate wall stresses and strains, and support understanding the mechanics of the vascular wall, as described in Bloksgaard, M. *et al*[13]. In this work, a mathematical model was applied to characterize the intrinsic stiffness of the elastin and collagen components of the arterial wall and to estimate the collagen recruitment strains[45,46] on the basis of calculated stress strain relationships. Imaging supported the findings from the mathematical modeling, that collagen in human resistance arteries was already recruited at low circumferential strain and wall stress. The quantitative measures of the microarchitecture of elastin and collagen described in this protocol can be further extended, inspired by the extensive work conducted on carotid arteries[6,8,47,48,49] and aorta[7,9,10,50,51]: additional analyses may include assessing the spatial distribution and microarchitecture of collagen and elastin fibers within the different layers of the arterial wall as well as fiber orientation angles (orientation with respect to the longitudinal axis). Bell *et al*.[15] addressed the pressure induced reorganization of the IEL and adventitial collagen including a multi-layer analytical model to calculate the stiffness and stress in each layer of the arterial wall. These authors[15] used human subcutaneous resistance arteries obtained from healthy volunteers, and related structure and wall stresses at 3 and 30 mmHg, respectively.

The proposed method in this protocol hopefully motivates further investigations and development of microstructurally motivated mathematical models for understanding the mechanical properties of human resistance arteries in health and disease. With further amendments of the method to include also collagen and elastin orientation angles along the longitudinal axis, smooth muscle cell volume density, spatial distribution and orientation within the arterial wall, collagen and elastin distribution and orientation in tunica media, and elastin organization and distribution in tunica adventitia, the imaging data can feed forward development of mathematical models, facilitating understanding of the remodeling process in hypertension, diabetes and the metabolic syndrome. Similarly, as suggested by Chen and Kassab for the coronary microcirculation[52,53], microstructure-based models of human resistance arteries can provide predictions of arterial mechanical responses at the macro- (whole artery) and micro-(structure) mechanical levels for each constituent. Such models must be based on quantitative data of structural parameters and mechanical properties of individual layers and constituents in the arterial wall of arteries originating from both healthy volunteers and patients suffering from different diseases, receiving different pharmacological treatments. Data are collected in a standardized manner and compared across individuals with different risk factor, disease and treatment profiles. The method has the potential to aid understanding how disease and medical treatments affect the human microcirculation.

Disclosures

The authors have nothing to disclose.

Acknowledgements

The authors thank the Danish Molecular Biomedical Imaging Center at the Faculty of Natural Sciences, University of Southern Denmark, for the use of laboratories and microscopes. Kristoffer Rosenstand and Ulla Melchior are acknowledged for excellent technical assistance with the pressure myography and imaging.

References

1. Briones, A. M., Arribas, S. M., & Salaices, M. Role of extracellular matrix in vascular remodeling of hypertension. *Curr Opin Nephrol Hy.* **19** (2), 187-194 (2010).
2. Heagerty, A. M., Heerkens, E. H., & Izzard, A. S. Small artery structure and function in hypertension. *J Cell Mol Med.* **14** (5), 1037-1043 (2010).
3. van den Akker, J., Schoorl, M. J., Bakker, E. N., & Vanbavel, E. Small artery remodeling: current concepts and questions. *J Vasc Res.* **47** (3), 183-202 (2010).
4. Rizzoni, D., & Agabiti-Rosei, E. Structural abnormalities of small resistance arteries in essential hypertension. *Intern Emerg Med.* **7** (3), 205-212 (2012).
5. Schiffrin, E. L. Vascular remodeling in hypertension: mechanisms and treatment. *Hypertension.* **59** (2), 367-374 (2012).
6. Fonck, E. *et al.* Effect of elastin degradation on carotid wall mechanics as assessed by a constituent-based biomechanical model. *Am J Physiol-Heart C.* **292** (6), H2754-2763 (2007).

7. Chow, M. J., Turcotte, R., Lin, C. P., & Zhang, Y. Arterial extracellular matrix: a mechanobiological study of the contributions and interactions of elastin and collagen. *Biophys J.* **106** (12), 2684-2692 (2014).
8. Chen, H. *et al.* Biaxial deformation of collagen and elastin fibers in coronary adventitia. *J Appl Physiol (1985).* **115** (11), 1683-1693 (2013).
9. Schriefl, A. J., Schmidt, T., Balzani, D., Sommer, G., & Holzapfel, G. A. Selective enzymatic removal of elastin and collagen from human abdominal aortas: uniaxial mechanical response and constitutive modeling. *Acta Biomater.* **17** 125-136 (2015).
10. Zeinali-Davarani, S., Wang, Y., Chow, M. J., Turcotte, R., & Zhang, Y. Contribution of collagen fiber undulation to regional biomechanical properties along porcine thoracic aorta. *J Biomech Eng.* **137** (5), 051001 (2015).
11. Mattson, J. M., Turcotte, R., & Zhang, Y. Glycosaminoglycans contribute to extracellular matrix fiber recruitment and arterial wall mechanics. *Biomech Model Mechan.* **16** (1), 213-225 (2017).
12. Schriefl, A. J., Zeindlinger, G., Pierce, D. M., Regitnig, P., & Holzapfel, G. A. Determination of the layer-specific distributed collagen fibre orientations in human thoracic and abdominal aortas and common iliac arteries. *J R Soc Interface.* **9** (71), 1275-1286 (2012).
13. Bloksgaard, M. *et al.* Imaging and modeling of acute pressure-induced changes of collagen and elastin microarchitectures in pig and human resistance arteries. *Am J Physiol-Heart C.* ajpheart 00110 02017 (2017).
14. Dora, K. A. *et al.* Isolated Human Pulmonary Artery Structure and Function Pre- and Post-Cardiopulmonary Bypass Surgery. *J Am Heart Assoc.* **5** (2) (2016).
15. Bell, J. S. *et al.* Microstructure and mechanics of human resistance arteries. *Am J Physiol-Heart C.* **311** (6), H1560-H1568 (2016).
16. Roque, F. R. *et al.* Aerobic exercise reduces oxidative stress and improves vascular changes of small mesenteric and coronary arteries in hypertension. *Brit J Pharmacol.* **168** (3), 686-703 (2013).
17. Briones, A. M. *et al.* Alterations in structure and mechanics of resistance arteries from ouabain-induced hypertensive rats. *Am J Physiol-Heart C.* **291** (1), H193-201 (2006).
18. Briones, A. M. *et al.* Role of elastin in spontaneously hypertensive rat small mesenteric artery remodelling. *J Physiol.* **552** (Pt 1), 185-195 (2003).
19. Arribas, S. M. *et al.* Confocal myography for the study of hypertensive vascular remodelling. *Clin Hemorheol Micro.* **37** (1-2), 205-210 (2007).
20. Gonzalez, J. M. *et al.* Postnatal alterations in elastic fiber organization precede resistance artery narrowing in SHR. *Am J Physiol-Heart C.* **291** (2), H804-812 (2006).
21. Spronck, B., Megens, R. T., Reesink, K. D., & Delhaas, T. A method for three-dimensional quantification of vascular smooth muscle orientation: application in viable murine carotid arteries. *Biomech Model Mechan.* **15** (2), 419-432 (2015).
22. Megens, R. T. *et al.* In vivo high-resolution structural imaging of large arteries in small rodents using two-photon laser scanning microscopy. *J Biomed Opt.* **15** (1), 011108 (2010).
23. Megens, R. T., oude Egbrink, M. G., Merkx, M., Slaaf, D. W., & van Zandvoort, M. A. Two-photon microscopy on vital carotid arteries: imaging the relationship between collagen and inflammatory cells in atherosclerotic plaques. *J Biomed Opt.* **13** (4), 044022 (2008).
24. Bender, S. B. *et al.* Regional variation in arterial stiffening and dysfunction in Western diet-induced obesity. *Am J Physiol-Heart C.* **309** (4), H574-582 (2015).
25. Clifford, P. S. *et al.* Spatial distribution and mechanical function of elastin in resistance arteries: a role in bearing longitudinal stress. *Arterioscler Thromb.* **31** (12), 2889-2896 (2011).
26. Martinez-Revelles, S. *et al.* Lysyl Oxidase Induces Vascular Oxidative Stress and Contributes to Arterial Stiffness and Abnormal Elastin Structure in Hypertension: Role of p38MAPK. *Antioxid Redox Sign.* **27** (7), 379-397 (2017).
27. Foote, C. A. *et al.* Arterial Stiffening in Western Diet-Fed Mice Is Associated with Increased Vascular Elastin, Transforming Growth Factor-beta, and Plasma Neuraminidase. *Front Physiol.* **7** 285 (2016).
28. Schindelin, J. *et al.* Fiji: an open-source platform for biological-image analysis. *Nat Methods.* **9** (7), 676-682 (2012).
29. Sommer, C., Straehle, C., Kothe, U., & Hamprecht, F. A. Ilastik: Interactive Learning and Segmentation Toolkit. *2011 8th Ieee International Symposium on Biomedical Imaging: From Nano to Macro.* 230-233 (2011).
30. Campagnola, P. J. *et al.* Three-dimensional high-resolution second-harmonic generation imaging of endogenous structural proteins in biological tissues. *Biophys J.* **82** (1 Pt 1), 493-508 (2002).
31. Intengan, H. D., Deng, L. Y., Li, J. S., & Schiffrin, E. L. Mechanics and composition of human subcutaneous resistance arteries in essential hypertension. *Hypertension.* **33** (1 Pt 2), 569-574 (1999).
32. Saatchi, S. *et al.* Three-dimensional microstructural changes in murine abdominal aortic aneurysms quantified using immunofluorescent array tomography. *J Histochem Cytochem.* **60** (2), 97-109 (2012).
33. Bloksgaard, M. *et al.* Elastin Organization in Pig and Cardiovascular Disease Patients' Pericardial Resistance Arteries. *J Vasc Res.* **52** (1), 1-11 (2015).
34. World Medical, A. World Medical Association Declaration of Helsinki: ethical principles for medical research involving human subjects. *JAMA.* **310** (20), 2191-2194 (2013).
35. Schneider, C. A., Rasband, W. S., & Eliceiri, K. W. NIH Image to ImageJ: 25 years of image analysis. *Nat Methods.* **9** (7), 671-675 (2012).
36. Meijering, E. *et al.* Design and validation of a tool for neurite tracing and analysis in fluorescence microscopy images. *Cytometry A.* **58** (2), 167-176 (2004).
37. Rezakhaniha, R. *et al.* Experimental investigation of collagen waviness and orientation in the arterial adventitia using confocal laser scanning microscopy. *Biomech Model Mechan.* **11** (3-4), 461-473 (2012).
38. Green, E. M., Mansfield, J. C., Bell, J. S., & Winlove, C. P. The structure and micromechanics of elastic tissue. *Interface Focus.* **4** (2), 20130058 (2014).
39. Bell, J. S. *et al.* Microstructure and mechanics of human resistance arteries. *Am J Physiol-Heart C.* **311** (6), H1560-H1568 (2016).
40. Shen, Z., Lu, Z., Chhatbar, P. Y., O'Herron, P., & Kara, P. An artery-specific fluorescent dye for studying neurovascular coupling. *Nat Methods.* **9** (3), 273-276 (2012).
41. Megens, R. T. *et al.* Imaging collagen in intact viable healthy and atherosclerotic arteries using fluorescently labeled CNA35 and two-photon laser scanning microscopy. *Mol Imaging.* **6** (4), 247-260 (2007).
42. Staiculescu, M. C. *et al.* Prolonged vasoconstriction of resistance arteries involves vascular smooth muscle actin polymerization leading to inward remodelling. *Cardiovasc Res.* **98** (3), 428-436 (2013).
43. Fung, Y. C., & Sobin, S. S. The retained elasticity of elastin under fixation agents. *J Biomech Eng.* **103** (2), 121-122 (1981).
44. Fung, Y. C. *Biomechanics : mechanical properties of living tissues.* 2nd edn, Springer-Verlag, (1993).
45. Bakker, E. N. *et al.* Heterogeneity in arterial remodeling among sublines of spontaneously hypertensive rats. *PLoS One.* **9** (9), e107998 (2014).

46. VanBavel, E., Siersma, P., & Spaan, J. A. Elasticity of passive blood vessels: a new concept. *Am J Physiol-Heart C.* **285** (5), H1986-2000 (2003).
47. Chen, H. *et al.* Microstructural constitutive model of active coronary media. *Biomaterials.* **34** (31), 7575-7583 (2013).
48. Saez, P., Garcia, A., Pena, E., Gasser, T. C., & Martinez, M. A. Microstructural quantification of collagen fiber orientations and its integration in constitutive modeling of the porcine carotid artery. *Acta Biomater.* **33** 183-193 (2016).
49. Bellini, C., Ferruzzi, J., Roccabianca, S., Di Martino, E. S., & Humphrey, J. D. A microstructurally motivated model of arterial wall mechanics with mechanobiological implications. *Ann Biomed Eng.* **42** (3), 488-502 (2014).
50. Schriefl, A. J., Wolinski, H., Regitnig, P., Kohlwein, S. D., & Holzapfel, G. A. An automated approach for three-dimensional quantification of fibrillar structures in optically cleared soft biological tissues. *J R Soc Interface.* **10** (80), 20120760 (2013).
51. Weisbecker, H., Unterberger, M. J., & Holzapfel, G. A. Constitutive modelling of arteries considering fibre recruitment and three-dimensional fibre distribution. *J R Soc Interface.* **12** (105), 20150111 (2015).
52. Chen, H., & Kassab, G. S. Microstructure-based biomechanics of coronary arteries in health and disease. *J Biomech.* **49** (12), 2548-2559 (2016).
53. Chen, H., & Kassab, G. S. Microstructure-based constitutive model of coronary artery with active smooth muscle contraction. *Sci Rep.* **7** (1), 9339 (2017).

